ISSN 1674-1056
http://cpb.iphy.ac.cn
http://iopscience.iop.org/cpb
中国物理 B
Chinese Physics
中国物理 Chinese Physics B

Observation of double pseudowaves in an ion-beam-plasma system

Zi-an Wei(卫子安), Jin-Xiu Ma(马锦秀), Kai-Yang Yi(弋开阳)

Citation: Chin. Phys. B . 2018, 27(8): 085201. **doi:** 10.1088/1674-1056/27/8/085201

Journal homepage: http://cpb.iphy.ac.cn; http://iopscience.iop.org/cpb

What follows is a list of articles you may be interested in

Upstream ion wave excitation in an ion-beam-plasma system

Kai-Yang Yi(弋开阳), Jin-Xiu Ma(马锦秀), Zi-An Wei(卫子安), Zheng-Yuan Li(李政元)

Chin. Phys. B . 2018, 27(5): 055201. **doi:** 10.1088/1674-1056/27/5/055201

Schamel equation in an inhomogeneous magnetized sheared flow plasma with *q*-nonextensive trapped electrons

Shaukat Ali Shan, Qamar-ul-Haque

Chin. Phys. B . 2018, 27(2): 025203. **doi:** 10.1088/1674-1056/27/2/025203

Plural interactions of space charge wave harmonics during the development of two-stream instability

Victor Kulish, Alexander Lysenko, Michael Rombovsky, Vitaliy Koval, Iurii Volk

Chin. Phys. B . 2015, 24(9): 095201. **doi:** 10.1088/1674-1056/24/9/095201

Kadomtsev–Petviashvili equation for dust ion-acoustic solitons in pair-ion plasmas

Hafeez Ur-Rehman

Chin. Phys. B . 2013, 22(3): 035202. **doi:** 10.1088/1674-1056/22/3/035202

Observation of double pseudowaves in an ion–beam–plasma system*

Zi-An Wei(卫子安), Jin-Xiu Ma(马锦秀)†, and Kai-Yang Yi(弋开阳)

Department of Modern Physics and CAS Key Laboratory of Geospace Environment, University of Science and Technology of China, Hefei 230026, China

(Received 19 April 2018; revised manuscript received 11 May 2018; published online 25 July 2018)

Pseudowaves, known as burst-ion signals, which are different from plasma normal modes, exist frequently in ion–wave excitation experiments when launching the waves by applying a pulsed voltage to a negatively biased grid. In previous experiments, only one kind of the pseudowave was observed. In this paper, we report the observation and identification of double pseudowaves in an ion–beam–plasma system. These pseudowaves originate from two ion groups: the burst of the beam ions and the burst of the background ions. It was observed that the burst of the background ions was in the case of high ion beam energy, while the burst of the beam ions was in the case of low ion beam energy. By observing the dependence of the signal velocities on the characteristics of the excitation voltage, these pseudowaves can be identified. It was also observed that the burst ion signal originating from the background ions can interact with slow beam mode and that originating from the beam ions can interact with fast beam mode.

Keywords: ion–beam–plasma system, normal modes, pseudowaves, wave–particle interaction

PACS: 52.35.–g, 52.35.Fp, 52.35.Qz, 52.20.–j **DOI:** 10.1088/1674-1056/27/8/085201

1. Introduction

Beam–plasma systems are paradigms exhibiting kinetic instabilities, which have important applications in many fields.[1,2] The waves and instabilities in such systems are of great interest to researchers in basic plasma physics and space plasmas. In an ion–beam–plasma system, the plasma normal (electrostatic) modes include a fast and a slow ion–beam mode and a background ion-acoustic mode.[3–5] The instabilities and nonlinear evolutions of the normal modes (solitons and shocks, etc.) in the ion–beam–plasma systems have been widely investigated during the past decades.[6–19] In the systems containing low-energy ion beams, the beam–plasma instabilities occur in a range of the beam Mach number (usually below 2–3)[10] and the instabilities are due to the wave–wave coupling between the slow beam mode and the ion–acoustic mode.

In ion–acoustic wave excitation experiments without ion beams, when the waves were launched by applying a pulsed voltage to an excitation grid, a kind of pseudowave signal was often observed to coexist with the excited ion–acoustic wave.[20] This signal looks like a wave signal propagating with its own velocity (usually faster than the ion–acoustic wave), but is not the normal mode of the plasma because it does not satisfy the dispersion relation, and thus was termed "pseudowave". The pseudowave signal appears only when launching the ion–acoustic wave with the partially transparent excitation grid (not nontransparent plate) and was attributed to the ions bursting out of the sheaths of the excitation grid when the sheath potential was rapidly raised because of the application of the excitation voltage.[21–23] It was also known as the burst-ion signal consisting of a pulsed ion beam released from the sheaths of the grid.[20–23] The signal velocity of the pseudowave (or burst-ions) depends sensitively on the characteristics of the excitation voltage (boundary condition),[21,24] which is totally different from the normal mode whose velocity is determined by the dispersion relation. By controlling the excitation voltage, the burst-ion velocity can be adjusted close to the velocity of the ion–acoustic wave. Thus, it is possible to observe the wave–particle interaction process. For instance, the coupling between the burst-ions and the ion–acoustic wave can result in the amplification of the latter and the formation of the ion–acoustic solitons and shocks.[24–26] However, the observation of the pseudowaves were not reported in previous wave-excitation experiments conducted in ion–beam–plasma systems.

Recently, in the wave-excitation experiment conducted in an ion–beam–plasma system, a kind of burst-ion signal was observed and identified to coexist with the plasma normal modes both in downstream[27] and in upstream[28] directions. These burst-ions signals only represent one kind of the pseudowaves that are produced from the background plasma.

In the present paper, we report the co-excitation of two kinds of the pseudowave signals moving in the downstream (along the beam) direction. These signals originate from two different ion groups: the beam and the background ions. It will be shown that the pseudowave signal arising from the background ions appear in the case of high beam energy while that arising from the beam ions appear in the case of low beam energy. In addition, the interactions between the pseudowave signals and the ion–beam modes have been observed.

*Project supported by the National Natural Science Foundation of China (Grant Nos. 11575183 and 11705201).

†Corresponding author. E-mail: jxma@ustc.edu.cn

© 2018 Chinese Physical Society and IOP Publishing Ltd

2. Experimental setup

The experiment was performed in a double plasma device 1000-mm long and 500 mm in diameter sketched in Fig. 1. The plasma was generated by hot-cathode discharge in the source chamber only and diffused (streamed) into the target chamber. The discharge voltage and current were kept at 30 V and 0.9 A, respectively. In the middle of the device, two adjacent separation grids SG1 and SG2 (60% transparency and 10-mm gap) were used to create the ion–beam–plasma system in the target chamber with controllable beam energy. A retarding field energy analyzer (RFEA) located 100 mm away from the SG2 was used to measure the ion velocity distribution function in the target chamber. The details can be found in Refs. [29] and [30]. The base pressure of the vacuum vessel was $p = 4 \times 10^{-4}$ Pa and the argon gas working pressure was kept at $p = 2.3 \times 10^{-2}$ Pa. The source chamber wall and the SG1 were grounded. Different from the experiments in Refs. [27] and [28], here the bias on the target chamber wall was kept at -40 V and the bias on the SG2, V_{SG2}, was varied to control the beam energy so that larger range of the beam energy (1.4 eV–21 eV) can be achieved.

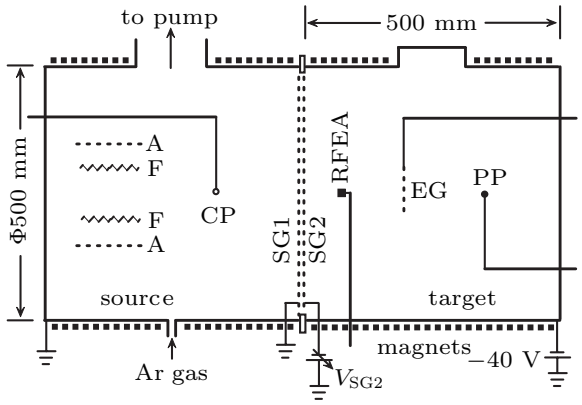


Fig. 1. Sketch of the experimental setup. A: anode, F: hot filaments; SG: separation grid; CP: cylindrical probe; PP: planar probe; EG: excitation grid; RFEA: retarding field energy analyzer.

A cylindrical probe (CP) was used to diagnose the plasma parameters in the source chamber, and a planar probe (PP, 10-mm diameter) was used both to diagnose the plasma parameters and to detect the wave signals in the target chamber. Typical electron density and temperature in the experimental region were $n_e \sim 5 \times 10^7$ cm^{-3} and $T_e \sim 1.2$ eV when the bias on SG2 was $V_{SG2} = -30$ V.

The beam energy was determined either from the RFEA data or by the difference between the plasma potentials in the source and experimental regions. Figure 2 shows the variations of the ion–beam energy, ε_b, and the density ratio of the beam to total ions, α, estimated from the RFEA data, with respect to V_{SG2}. When V_{SG2} is in the range of -42 V to -28 V, the beam energy increases monotonically with V_{SG2}, and α is about 0.7 and changes only slightly.

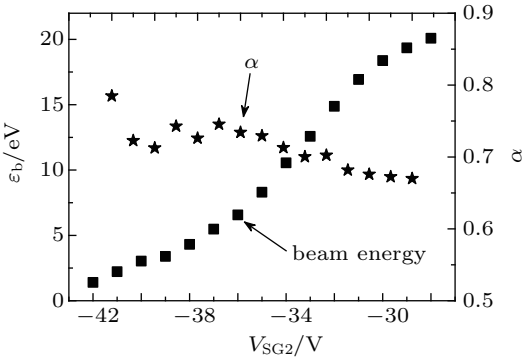


Fig. 2. The ion–beam energy, ε_b, and the density ratio between the beam and the total ions, α, versus V_{SG2}.

3. Lauching of the waves

The waves were launched by applying a ramp voltage to a negatively-biased excitation grid (EG, 80 mm in diameter, 65% transparency) located at 200 mm from the SG2. The voltage on the EG is

$$V_{EG} = -52 + V_{pp} \tanh(t/\tau) \,, \tag{1}$$

where V_{pp} and τ are the peak-to-peak amplitude and rise time of the ramp signal, which are the two controlling parameters

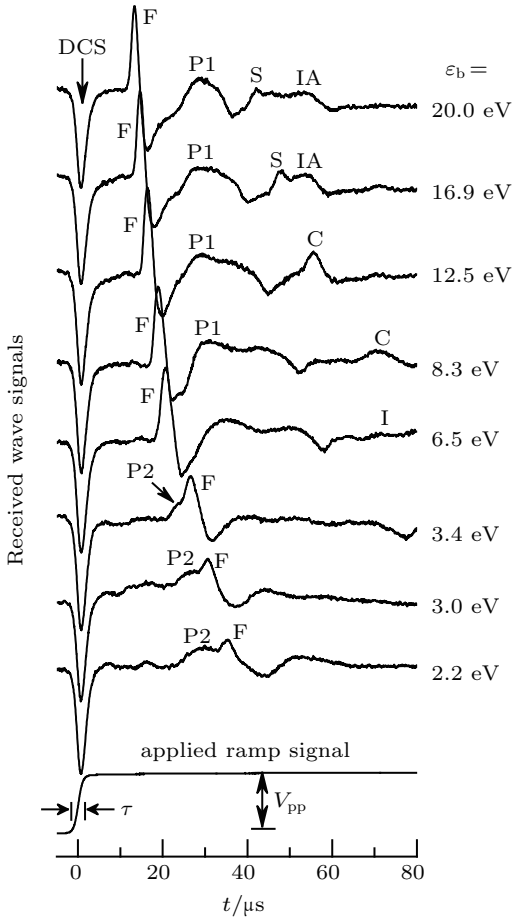


Fig. 3. Evolutions of the wave signals with respect to the ion–beam energy ε_b, received at 123 mm from the excitation grid in the case of $V_{pp} = 16$ V and $\tau = 3.59$ μs. DCS: directly coupled signal; F: fast beam mode; S: slow beam mode; IA: ion–acoustic mode; C: coupled signal; I: instability; P1 and P2: first and second pseudowave signals.

of the excitation voltage. The excited wave signals were detected by measuring the perturbations in the electron density (approximately equal to the ion density perturbation because of the quasi-neutrality) with the planar probe and were monitored on a digital oscilloscope.

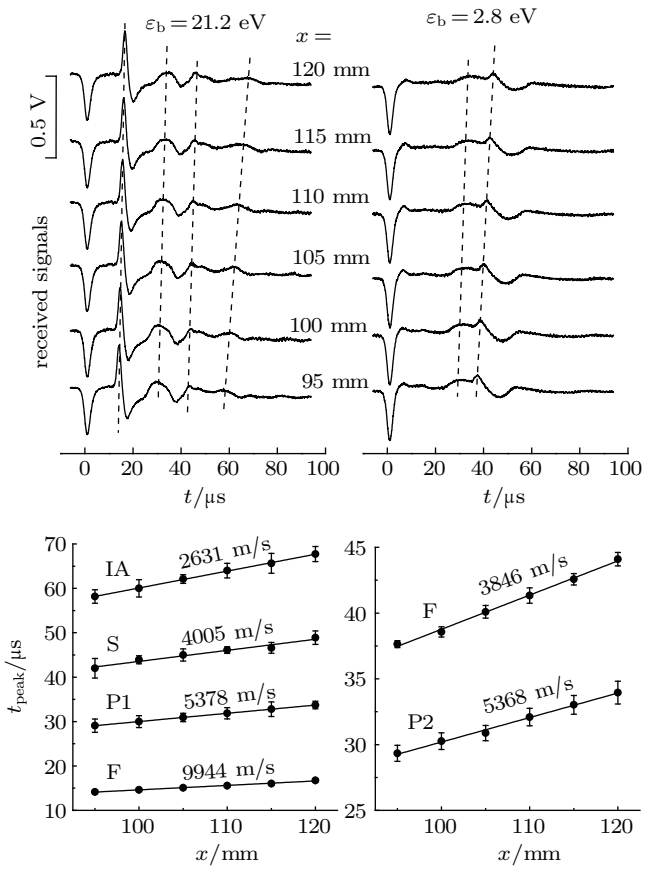


Fig. 4. Upper parts: trajectories of the received signals with respect to the distance from the excitation grid. Lower parts: time-of-flight graph for the received signals (peak time versus distance). Left column: $\varepsilon_b = 21.2$ eV. Right column: $\varepsilon_b = 2.8$ eV. The dashed lines indicate the trajectories of the signal peaks. $V_{pp} = 20$ V and $\tau = 4.31$ μs.

Different from the previous observations,[27,28] here we observed two kinds of pseudowaves, depending on the beam energy. Figure 3 shows the evolutions of the received signals, detected at 123 mm from the EG (the signals are well separated at this distance), with respect to the beam energy for a given excitation voltage with $\tau = 3.59$ μs and $V_{pp} = 16$ V. In the case of high beam energy ($\varepsilon_b = 20$ eV), the three normal modes (to be identified later) were observed, i.e., the fast beam mode (F), the slow beam mode (S), and the background ion–acoustic mode (IA). In addition, a pseudowave signal P1 appears between the F and S signals, which is the burst ion signal originating from the background ions. As ε_b decreases, the signals F and S move rightwards (i.e., their velocities decrease), but the signal IA moves little, so that the signal S approaches to the signal IA and at $\varepsilon_b \sim 12.5$ eV these two signals merge into a coupled signal C. Further decrease of ε_b results in the slow down and decay of the signal C, and when $\varepsilon_b \sim 6.5$ eV the coupled signal evolves into an instability (not obvious). When ε_b is below 3.4 eV, the second pseudowave signal P2 emerges in front of the signal F. The signal P2 was not observed previously and is resulted from the burst ions that originate from the ion beam.

Figure 4 shows the trajectories of the received signals with respect to the distance from the excitation grid for the cases of two different beam energies. The signal propagation velocity can be obtained using the time-of-flight (TOF) method from these trajectories. In the case of high beam energy when $\varepsilon_b = 21.2$ eV, the four propagating signals, i.e., signal F, P1, S, and IA, with different velocities (shown in the TOF graph in the lower parts of Fig. 4) can be easily seen. In the case of low beam energy when $\varepsilon_b = 2.8$ eV, only two propagating signals, i.e., signal P2 and F, with different velocities can be obviously observed.

4. Identification of the waves

The plasma normal modes can be identified by observing the fact that the signal velocities are independent of the characteristics (i.e., V_{pp} and τ) of the ramp excitation voltage but depend on the beam energy. Their velocities are determined by the wave dispersion relations. The pseudowaves or burst-ion signals, on the other hand, can be identified from the property that the signal velocities depend sensitively on V_{pp} and τ.[27,28]

In order to confirm that the signal P1 and P2 are the burst-ion signals, but the signal F, S, and IA are the plasma normal modes, we present in Fig. 5 the signal velocities versus τ and V_{pp} in the cases of high beam energy $\varepsilon_b = 21$ eV ((a) and (b)) and low beam energy $\varepsilon_b = 3.2$ eV ((c) and (d)), respectively. The results show that, the velocities of the F, S, and IA signals do not vary with τ and V_{pp}, indicating that they are the plasma normal modes, whereas the velocities of the P1 and P2 signals decrease with the increase of τ and increase with the increase of V_{pp}. Thus, the properties of the P1 and P2 signals are in agreement with the characteristics of the burst ions.[22,26,27]

To further identify the signals, we plot the signal velocities versus the ion–beam energy in Fig. 6 for the given V_{pp} and τ. It is shown that the velocities of the signal F and S increase with the increase of ε_b, indicating that they are fast and slow beam modes. The velocities of the signals IA, C, and I change very little, indicating that they are ion–acoustic modes. The velocity of the signal P2 increases with ε_b, indicating that it originates from the beam ions. The variation of the velocity of the signal P1 is not obvious, indicating that it is related to the background ions.

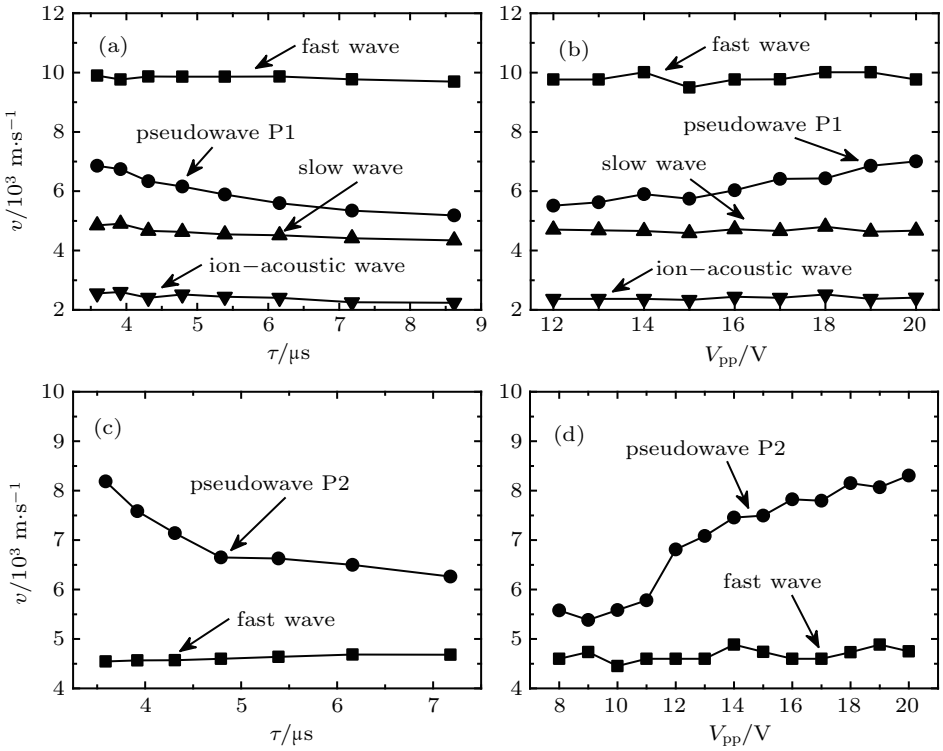


Fig. 5. Signal velocities versus: (a) and (c), τ when $V_{pp} = 20$ V and $\varepsilon_b = 20$ eV ($V_{SG2} = -28$ V); and (b) and (d), V_{pp} when $\tau = 4.31$ μs and $\varepsilon_b = 3.2$ eV ($V_{SG2} = -40$ V).

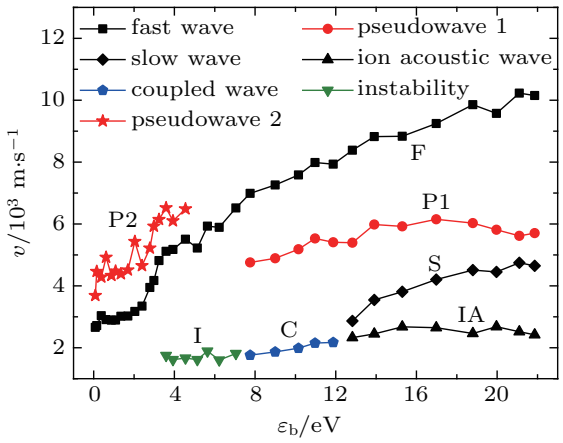


Fig. 6. (color online) Signal velocities versus the beam energy. $\tau = 4.31$ μs and $V_{pp} = 20$ V.

To qualitatively explain the observed phenomena, we use the simplest model to determine the phase velocities (same as the group or signal velocities in this case) of the plasma normal modes in the ion–beam–plasma system. In the plasma containing a monoenergetic ion beam, the normal modes propagating in the downstream (along the beam) direction are well know to be the fast and slow beam modes and the ion–acoustic mode.[3–5] The phase velocities for the fast and slow ion–beam modes are[27]

$$v_{F,S} \sim v_b \pm \alpha^{1/2} c_s, \tag{2}$$

and that for the ion–acoustic wave is[27]

$$v_{IA} \sim (1-\alpha)^{1/2} c_s, \tag{3}$$

where v_b is the ion–beam velocity, α is the ratio between the ion–beam density and the total ion density, $c_s = (T_e/m_i)^{1/2}$ is the ion–acoustic speed, and m_i is the ion mass. It shows that v_F and v_S are roughly proportional to v_b while v_{IA} is roughly independent of v_b. This is in qualitative agreement with the experimental observations. Here, the fast and slow waves can also be regarded as the ion acoustic waves riding on the stationary ion beam launched at the separation grids of the double-plasma device.

The burst ions are those originating in the sheath regions of the excitation grid and accelerated by the rapidly raised sheath potential because of the application of the ramp excitation voltage. Without the application of the ramp voltage to the EG, the beam ions together with the background ions in the upstream side of the EG will stream into the upstream sheath, transit through, and exit out of the downstream sheath of the EG, with the energy the same as the incident energy because of the energy conservation. With the application of the ramp voltage to the EG, the sheath potentials will be rapidly raised because the sheaths do not have sufficient time to relax. The ions originally in the sheath regions will be rapidly accelerated because of the energy conservation. These ions will burst out of the sheath region with an energy increase., i.e., they behave as a pulsed ion beam. In the downstream direction, these burst ions consist two groups: the beam and the background, since the original ions moving from the upstream to the downstream direction in the sheath regions contain these two components. This case is opposed to the case for the burst-

ions in the upstream direction where there is only background group[28] (i.e., no burst ions originating from the beam ions moving from the downstream to the upstream direction, since the ion beam only move from the upstream to the downstream direction). The average velocity of the burst ions can be approximated by[26]

$$v_{\mathrm{BI}} \sim c_{\mathrm{s}} \left(M^2 + \frac{2eV_{\mathrm{pp}}}{T_{\mathrm{e}}} \frac{1}{f_{\mathrm{pi}}\tau} \right)^{1/2}, \tag{4}$$

where M is the ion Mach number in the bulk plasma, e is the ion charge, and f_{pi} is the ion plasma frequency. For the signal P1 due to the burst of the background ions, $M = 0$, and for the signal P2 due to the burst of the beam ions, $M = v_{\mathrm{b}}/c_{\mathrm{s}} = (2\varepsilon_{\mathrm{b}}/T_{\mathrm{e}})^{1/2}$, respectively.

Based on Eq. (4), the properties of the pseudowaves can be qualitatively understood. For the signal P1, $v_{\mathrm{P1}} \sim (2eV_{\mathrm{pp}}/m_{\mathrm{i}}f_{\mathrm{pi}}\tau)^{1/2}$, which increases with V_{pp} and decreases with τ but is independent of the ion–beam energy. This is in qualitative agreement with the experimental observations. For the signal P2, $v_{\mathrm{P2}} \sim (2\varepsilon_{\mathrm{b}}/m_{\mathrm{i}} + 2eV_{\mathrm{pp}}/m_{\mathrm{i}}f_{\mathrm{pi}}\tau)^{1/2}$. At high beam energies, the second term is less important than the first one, so that the velocity of the signal P2 is close to that of the signal F, thus, the two signals overlap and are hard to be distinguished. At low beam energies, the second term becomes important so that the the signal P2 is faster than the signal F, resulting in the separation of these signals. Furthermore, the velocity of the P2 increases with the increase of the ion–beam energy and the V_{pp} but decreases with the increase of τ, which is in qualitative agreement with the results in Figs. 5 and 6.

5. Pseudowave–normal-mode interactions

Both the equation (4) and the results in Fig. 5 shows that the signal velocities of the pseudowaves increases with the increase of V_{pp} and the decrease of τ. Since the pseudowaves are recognized as the pulsed beam of burst ions, it is possible to observe the wave–particle interactions between the normal modes and the burst ions when the burst-ion velocities are adjusted to be close to the normal mode velocities. Here, the most direct observation is to adjust the burst-ion velocities via the adjustment of the ramp voltage rise time τ.

At a high beam energy $\varepsilon_{\mathrm{b}} = 21$ eV, the interactions between the signals P1 and the S and IA can be observed. For a fixed $V_{\mathrm{pp}} = 10$ V, the variations of the signals and their peak values with respect to τ are shown in Fig. 7. At small value of $\tau = 4.31$ μs, the signals are well separated. As τ increases, the velocity of the signal P1 decreases and approaches to that of the signal S, causing the enhancement of the signal S due to the effect of the inverse Landau damping. Further increase of τ results in further decrease of the P1 velocity to a value between that of the signal S and IA (it is not easy to observe the signal P1 when it lies between the signal S and IA), causing the weakening of the signal S due to the effect of the Landau damping but the enhancement of the signal IA due to the effect of the inverse Landau damping, as is obvious from the signal peak value variations shown in Fig. 7(b). Thus, the successive interactions of the signal P1 with the signal S and IA have been observed.

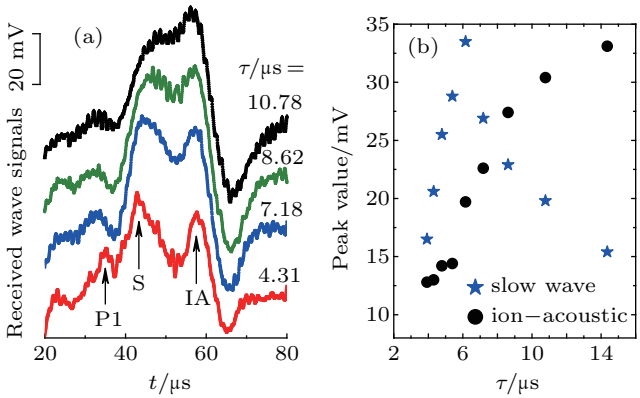


Fig. 7. (color online) (a) The dependence of the signals received at 140 mm from the excitation grid with respect to τ when $V_{\mathrm{pp}} = 10$ V, $V_{\mathrm{SG2}} = -28$ V, and $\varepsilon_{\mathrm{b}} = 20$ eV. (b) The peak value of the signals versus τ.

At a low beam energy $\varepsilon_{\mathrm{b}} = 3.2$ eV, the interactions between the signals P2 and F can be observed. The results are shown in Fig. 8. For a fixed value of $V_{\mathrm{pp}} = 12$ V, when $\tau = 2.69$ μs, the signal P2 appears in front of (faster than) the signal F. With the increase of τ, the velocity of the signal P2 decreases and approaches to that of the signal F, leading to significant enhancement of the signal F due to the effect of the inverse Landau damping.

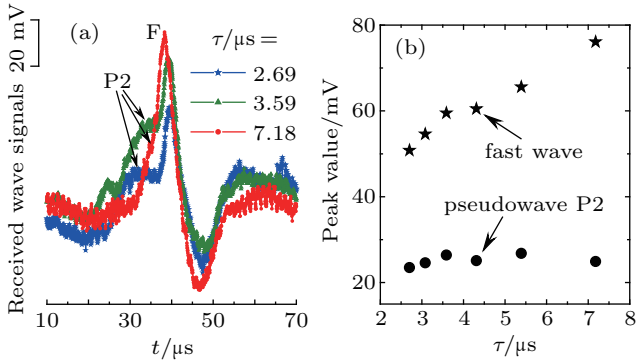


Fig. 8. (color online) (a) The dependence of the signals received at 140 mm from the excitation grid with respect to τ when $V_{\mathrm{pp}} = 12$ V, $V_{\mathrm{SG2}} = -40$ V, and $\varepsilon_{\mathrm{b}} = 3.2$ eV. (b) The peak value of the signals versus τ.

6. Summary

In summary, the two kinds of the pseudowaves and the three normal modes propagating in the downstream direction of the beam have been co-excited in the ion–beam–plasma system. The observed two kinds of the pseudowaves are the burst-ion signals with different originality: one from the background and the other from the beam ions. The burst-ion signal of the background-ion originality appears in the high beam energy case while that of the beam–ion originality appears in the low beam energy case. The burst-ion signals can be identified

by their velocity dependence on the excitation characteristics. The normal mode signals of the system can be identified because their velocities are independent of the excitation characteristics but determined by the dispersion relation. From the dependence of the signal velocities on the beam energy, the fast and the slow beam modes as well as the background ion–acoustic mode can be identified.

Utilizing the properties that the burst-ion velocities can be controlled by the rise time and peak-to-peak amplitude of the applied ramp voltage, the wave–particle interactions between the burst ions and the plasma normal modes can be observed. In the high beam-energy case, the successive interaction between the burst-ion signal originating from the background ions and the slow beam signal and the ion–acoustic signal has been inferred. In the high beam-energy case, the interaction between the burst-ion signal originating from the beam ions and the fast beam signal has been observed.

Acknowledgment

We acknowledge Fei Wu and Zhengyuan Li for their assistance in the experiment.

References

[1] Tokluoglu E and Kaganovich I D 2015 *Phys. Plasma* **22** 040701
[2] Kaganovich I D and Sydorenko D 2016 *Phys. Plasmas* **23** 112116
[3] Hershkowitz N, Romesser T, Knorr G and Goertz C K 1974 *Phys. Rev. Lett.* **33** 754
[4] Grésillon D and Doveil F 1975 *Phys. Rev. Lett.* **34** 77
[5] Sato N, Sugai H and Hatakeyama R 1975 *Phys. Rev. Lett.* **34** 931
[6] Fujita T, Ohnuma T and Adachi S 1975 *Phys. Fluids* **18** 1216
[7] Honzawa T 1984 *Phys. Rev. Lett.* **53** 1915
[8] Bonhomme G, Pierre T, Leclert G and Trulsen J 1991 *Plasma Phys. Control. Fusion* **33** 507
[9] Nagasawa T and Nishida Y 1994 *Phys. Rev. E* **49** 4442
[10] Lee S G, Diebold D A, Hershkowitz N and Moroz P 1996 *Phys. Rev. Lett.* **77** 1290
[11] Nagasawa T and Honzawa T 1996 *Phys. Plasmas* **3** 2864
[12] Nakamura Y and Komatsuda K 1998 *J. Plasma Phys.* **60** 69
[13] Franck C, Klinger T and Piel A 1999 *Phys. Lett. A* **259** 152
[14] Nakamura Y, Bailung H and Ichiki R 2004 *Phys. Plasmas* **11** 3795
[15] Sharma S K and Bailung H 2010 *Phys. Plasmas* **17** 032301
[16] Deka M K, Adhikary N C, Misra A P, Bailung H and Nakamura Y 2012 *Phys. Plasmas* **19** 103704
[17] Rapson C, Grulke O, Matyash K and Klinger T 2014 *Phys. Plasmas* **21** 052103
[18] Lotov K V, Timofeev I V, Mesyats E A, Snytnikov A V and Vshivkov V A 2015 *Phys. Plasmas* **22** 024502
[19] Koshkarov O, Smolyakov A I, Kaganovich I D and Ilgisonis V I 2015 *Phys. Plasmas* **22** 052113
[20] Alexeff I, Jones W D and Lonngren K E 1968 *Phys. Rev. Lett.* **21** 878
[21] Lonngren K E, Khazei M, Gabl E F and Bulson J M 1982 *Plasma Phys.* **24** 1483
[22] Gabl E F and Lonngren K E 1984 *Plasma Phys. Control. Fusion* **26** 799
[23] Raychaudhuri S, Gabl E F, Tsikis E K and Lonngren K E 1984 *Plasma Phys. Control. Fusion* **26** 1451
[24] Yi S, Bai E W and Lonngren K E 1997 *Phys. Plasmas* **4** 2436
[25] Honzawa T and Nagasawa T 1997 *Phys. Plasmas* **4** 3954
[26] Xiao D L, Ma J X, Li Y R, Li Y F and Yu M Y 2007 *Phys. Plasmas* **14** 092104
[27] Wu F, Ma J X, Wei Z A, Yi K Y and Wang T T 2016 *Phys. Plasmas* **23** 102118
[28] Yi K Y, Ma J X, Wei Z A and Li Z Y 2018 *Chin. Phys. B* **27** 055201
[29] Wei Z, Ma J, Li Y, Sun Y and Jiang Z 2016 *Plasma Sci. Technol.* **18** 1076
[30] Wei Z A and Ma J X 2016 *Phys. Plasmas* **23** 023502